Relationship between the microscopic morphology and the charge transport properties in poly(3-hexylthiophene) field-effect transistors

M. Surin,[a),b)] Ph. Leclère, and R. Lazzaroni
Chimie des Matériaux Nouveaux, Université de Mons-Hainaut, 20 Place du Parc, 7000 Mons, Belgium

J. D. Yuen, G. Wang, D. Moses,[a)] and A. J. Heeger
Center for Polymers and Organic Solids, University of California at Santa Barbara, Santa Barbara, California 93106-5090

S. Cho[b)] and K. Lee[b)]
Department of Physics, Pusan National University, Busan 609-735, Korea

(Received 2 February 2006; accepted 8 June 2006; published online 8 August 2006)

We fabricate field-effect transistors (FETs) by depositing a regioregular poly(3-hexylthiophene) (RR-P3HT) active layer via different preparation methods. The solvent used in the polymer film deposition and the deposition technique determine the film microstructure, which ranges from amorphous or granular films to a well-defined fibrillar texture. The crystalline ordering of RR-P3HT into fibrillar structures appears to lead to optimal FET performances, suggesting that fibrils act as efficient "conduits" for the charge carrier transport. Treating the silicon oxide gate insulator with hexamethyldisilazane enhanced the FET performance. © *2006 American Institute of Physics*.
[DOI: 10.1063/1.2222065]

I. INTRODUCTION

Organic field-effect transistors (OFETs) are attracting strong interest due to a number of attractive features amenable for fabricating low-cost, flexible electronic devices such as integrated circuits, electronic papers, smart tags, etc.[1] Additionally, from the fundamental standpoint, OFETs have been used for characterizing the charge transport properties, and in particular the charge carrier mobility, in organic semiconductors, a parameter which is fundamental for the understanding of the electronic processes in semiconductors.[2] A great effort has been devoted to conjugated polymers as FET active layers because of their easy processing via solution deposition techniques. In particular, polythiophene has appeared as the most promising polymer system as it exhibits the largest carrier mobility, in the range of 10^{-2}–10^{-1} $cm^2\,V^{-1}\,s^{-1}$, i.e., approaching that of amorphous silicon. This performance has been reached by "macromolecular engineering," i.e., by improving the regioregularity of the alkyl groups on the polythiophene backbone and increasing the polymer molecular weight.[3,4] Additional improvement has been made by exploring various aspects of the device preparation such as the active-layer film deposition technique,[5,6] the solvent used,[7] the nature of the dielectric substrate[8] (which may strongly influence the polymer structural order) which in turn affect the overall FET device performance.

It is worth nothing that, although significant progress has been made, some discrepancies appear in recent literature; for instance, Chang *et al.* suggest that the use of slowly evaporating solvents for spin coating the soluble polymer improves the structural order and thereby the FET performance as compared to films prepared from fast-evaporating solvents.[9] In contrast, Bao, Dodabalapur, and Lovinger suggest that when drop casting is used,[10] the best performances are obtained for fast-evaporating solvents such as chloroform.

The importance of the microscopic morphology of the polymer layer has been demonstrated in a few recent studies: for example, x-ray diffraction studies revealed that regular π stacking with the stacking direction in the plane of the film is important for obtaining efficient charge transport.[4,11] Nevertheless, at this stage only a few studies have focused specifically on the microstructure in the FET channel, and no consensus has yet been established as to the effect of the microscopic morphology on the charge transport in FET. For instance, Kline *et al.*[12] proposed that the self-assembly of regioregular poly(3-hexylthiophene) (RR-P3HT) into fibril-like structures leads to lower FET performance than homogeneous, featureless films made of higher molecular weight RR-P3HTs, whereas using dip coating of RR-P3HT solutions at various dipping speeds, Wang *et al.* concluded that the presence of such fibrillar morphology significantly enhances the performance (especially the charge mobility) compared to that of amorphous films.[13,14]

In order to elucidate the relationship between the performance of polymer FETs and the polymer structural features in the FET channel, we have systematically studied the morphology and the FET characteristics of a variety of thin film (in the 10–20 nm thickness range) FET made of RR-P3HT prepared in various solvents and with different deposition techniques. The microstructure was studied by means of tapping-mode atomic force microscopy (TM-AFM), which allowed probing of the thin film microstructure inside the FET channel (of 5 μm length) as well as the interfacial regions near the gold electrodes. Our studies were focused in particular on: (i) the comparison between the different pre-

[a)]Authors to whom correspondence should be addressed; electronic mail: moses@ipos.ucsb.edu; mathieu@averell.umh.ac.be
[b)]Also at University of California at Santa Barbara.

 © 2006 American Institute of Physics

Downloaded 15 Aug 2006 to 131.155.214.50. Redistribution subject to AIP license or copyright, see http://jap.aip.org/jap/copyright.jsp

paation methods: spin coating, drop casting and dip coating using different solvents; (ii) the influence of the dielectric substrate (gate insulator) over which the RR-P3HT solution was deposited. As is demonstrated in the following, this study provides an insight into the interplay between the charge transport properties, the microscopic morphology and the film preparation methods, which constitutes a firm basis for the fabrication of high-performance FET made of RR-P3HT.

II. EXPERIMENTAL APPROACHES

The FET substrates were prepared in a clean room using heavily doped (n^{++}) crystalline silicon wafer as the gate, over which a 200-nm-thick silicon oxide (SiO_2) layer (gate insulator) has been thermally grown (bottom gate configuration). The patterning of the bottom gold electrodes (grown over a 3-nm-thick titanium adhesion layer) was accomplished by standard photolithographic methods. Gold electrodes 50 nm thick were grown (by e-beam evaporation) on top of the doped silicon, in order to control the gate voltage. On each doped Si substrate, an array of FET was fabricated with channel lengths of 5 or 10 μm. Prior to deposition, the substrates were cleaned using a standard cleaning procedure (using different solvent treatments, and ozone plasma etching). Hexamethyldisilazane (HMDS) treatment of the substrates was done by soaking the FET substrates in HMDS for one day followed by the spin coating of a HMDS droplet at 4000 rpm for a duration of 60 s.

The RR-P3HT used in this study was obtained from Rieke Metals, Inc. (degree of regioregularity >98.5%).[3(b)] The film deposition parameters were set to produce ultrathin RR-P3HT films, i.e., in the range of 10–20 nm. Indeed, this thickness represents a few polymer monolayers; this allows us to compare the microscopic morphology within these layers and the device properties since it has been shown that in OFETs all the charge transport occurs within the first 2 ML of the active material channel, near the dielectric layer.[2(b)] This thickness regime has been achieved using the following procedures:

Dip coating: polymer solution concentration $=1.0$ mg/ml; dip speed $=1$ mm/min.
Drop casting: polymer solution concentration $=0.1$ mg/ml; 10 μl droplet.
Spin coating: polymer solution concentration $=1.0$ mg/ml; spin speed $=4000$ rpm, during 60 s.

The electrical measurements were carried out at room temperature under a nitrogen environment (in a glovebox) using a Keithley semiconductor parametric analyzer (Keithley 4200).

Tapping-mode AFM was performed with Nanoscope IIIa and Dimension 3100 microscopes from Veeco (operating in air, at room temperature). Microfabricated silicon cantilevers were used with a spring constant of ~ 30 N m^{-1}. Images of different areas of the samples were collected with the maximum available number of pixels (512) in each direction. The Nanoscope III v5.12 image processing software was used for image analysis.

III. RESULTS AND DISCUSSION

Spin coating, drop casting, and dip coating are the three major solution-based thin film preparation methods. In the first method, a droplet of solution is deposited to cover the whole substrate surface, followed by a spinning process at a controlled speed. Drop casting is the deposition of a droplet of controlled volume followed by the evaporation of the solvent; this process is similar to what happens in ink-jet printing. Dip coating consists of the dipping of the substrate in a solution followed by the vertical withdrawal of the sample at a controlled speed. We have employed these three processing techniques using three different solvents for dissolving RR-P3HT which span a large range in terms of evaporation speed: (i) chloroform (fast evaporation rate, boiling point $=61$°C; vapor pressure at room temperature=159 mmHg), (ii) *p*-xylene (intermediate evaporation rate, boiling point $=138.3$ °C; vapor pressure$=6.5$ mmHg), and (iii) 1,2,4-trichlorobenzene ("TCB," very slow evaporation rate, boiling point$=213$ °C; vapor pressure$=0.29$ mmHg). This choice of solvents was particularly useful for determining the effect of the evaporation rate of the solvent on the time scale of the film-forming process.

The characteristics of the FET were examined in the accumulation regime of hole transport (i.e., negative gate-source voltage), since holes are the major charge carrier in oligo- and polythiophenes using this type of device architecture (the highest occupied molecular orbital energy of P3HT is around 4.9 eV and the work function of gold is 5.1 eV). In contrast, electron injection and mobility are inhibited due to the large barrier at the gold electrode-polymer interface (the lowest unoccupied molecular orbital energy of P3HT is around 2.7 eV) and to electron trapping at the dielectric surface. Note that electron transport in polymer FET has been recently achieved by Chua *et al.*[15] by compensating the traps in the SiO_2 gate insulator; nevertheless, the electron mobility (on the order of 10^{-4} cm^2 V^{-1} s^{-1}) remains a few orders of magnitude lower than the best reported hole mobilities (10^{-2}–10^{-1} cm^2 V^{-1} s^{-1}).

Figure 1 (top panel) depicts a typical set of I_{ds}-V_{ds} curves for a FET device fabricated using spin coating from TCB solution. Generally, the data indicate a good on/off ratio and, for devices prepared from different preparation methods (deposition technique, solvent), we observe rather large variations in the source-drain current, from a few μA to a few mA, at $V_{gs}=V_{ds}=-60$ V. In the example shown in Fig. 1, the transfer characteristics (bottom graph) measured at constant $V_{ds}=-60$ V, show: (i) a relatively small threshold voltage, which indicates a rather low level of doping of the RR-P3HT; (ii) a little hysteresis, which indicates a low density of traps. We measured many different FETs for a given process/solvent, and in Table I we summarize the average current on/off ratios (i.e., the ratios of the current at $V_{gs}=-60$ V and

Downloaded 15 Aug 2006 to 131.155.214.50. Redistribution subject to AIP license or copyright, see http://jap.aip.org/jap/copyright.jsp

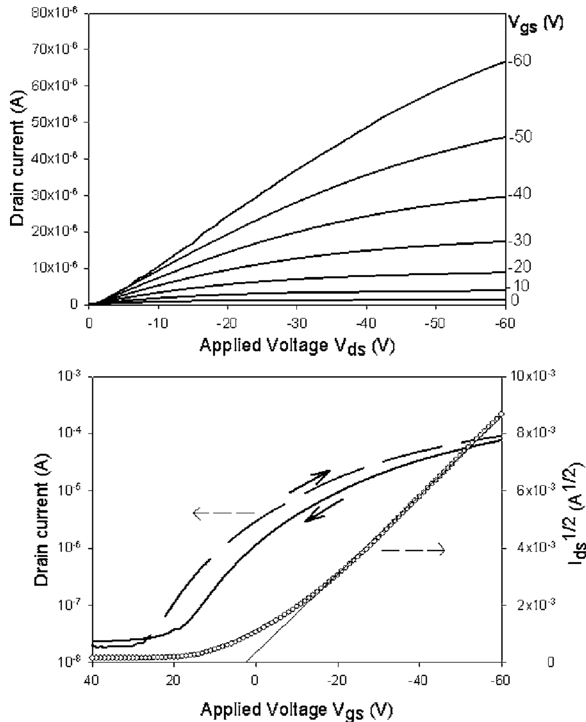

FIG. 1. Example of output (top) and transfer (bottom, $V_{ds}=-60$ V) characteristics for FET made of thin RR-P3HT films (here prepared by spin coating from TCB). ($I_{ds}^{1/2}$ vs V_{gs} graph: open circles =experimental data; solid black line =fit line).

the current at $V_{gs}=0$ V) and average the hole mobility μ, determined in the saturation regime ($V_{ds}=-60$ V), using the equation

$$I_{ds} = \frac{WC_i}{2L}\mu(V_{gs} - V_T)^2,$$

where W and L are the channel width (1000 μm) and length (5 or 10 μm), respectively, C_i is the capacitance of the SiO_2 dielectric ($C_i=15$ nF/cm^2), V_T the threshold voltage (V). The carrier mobility μ (cm^2 V^{-1} s^{-1}) is calculated by determining the slope of $I_{ds}^{1/2}$ vs V_{gs}. The method is strictly valid when the charge mobility is independent of V_{gs}; although a quite good linearity is observed in all cases when plotting $I_{ds}^{1/2}$ vs V_{gs}, the mobility values in Table I have to be considered as average values at highly negative values of V_{gs}.

From Table I it appears that different preparation conditions result in variations over three orders of magnitude in both the carrier mobility and on/off ratio. The highest carrier mobility of $\sim$0.085 cm^2 V^{-1} s^{-1} was found for films prepared using dip coating from polymer solutions in chloroform, while the lowest mobility is obtained for drop-cast films prepared using the TCB solvent ($\sim 10^{-4}$ cm^2 V^{-1} s^{-1}). When comparing the magnitude of the carrier (hole) mobility along a given column in Table I, we observe that, for devices fabricated using dip coating and drop casting, the general trend is an increase in the performances for the rapidly evaporating solvents, but the opposite trend is observed for films prepared by spin coating. In terms of current on/off ratio, the dip-coating process results in the highest values, which are a few orders of magnitude larger than those obtained for drop-cast films. We note that drop-cast films showed large performance variations, apparently as a consequence of the nonuniformity of the deposits; in contrast, both dip coating and spin coating result in uniform and homogeneous films.

The data in Table I suggest that the film-formation process, which determines the film microstructure, is quite different for the different deposition methods (e.g., dip coating and drop casting as compared to spin coating). Therefore, a careful investigation of the microscopic morphology, within the FET channels, has been carried out for each sample, by means of TM-AFM.

The TM-AFM images in Fig. 2 show that dip coating from polymer/TCB solutions leads to untextured, homogeneous films while films prepared from chloroform [Fig. 2(b)] and *p*-xylene [Fig. 2(c)] show a well-defined fibrillar morphology. In the latter two cases, the length of the fibrils varies from a few hundreds nm to a few μm, while their width and height remain uniform (about 20 and 35 nm, respectively); at the microscopic level, the deposits are made of a web of randomly oriented fibrils. This fibrillar morphology is the signature of the crystalline ordering of RR-P3HT chains, where each single fibril is made of π-stacked chains with the backbone axis perpendicular to the fibril axis (the stacking direction), as suggested by structural studies using x-ray diffraction.[14,16] Each fibril corresponds to a crystalline lamella, with an interchain distance of 0.38 nm (stacking distance between thiophene backbones) and an interlamellar distance around 1.7 nm (due to interdigitation of hexyl

TABLE I. Average hole mobility (μ, cm^2 V^{-1} s^{-1}) and current on/off ratio (I on/off) of RR-P3HT FET using different preparation methods and different solvents. Since the values have been determined testing different FETs, the errors on the charge mobility values are noted below each value.

Solvent/Process	Dip coating		Drop casting		Spin coating	
	μ	I on/off	μ	I on/off	μ	I on/off
TCB (b.p. 213 °C)	2.4×10^{-3} ($\pm0.7\times10^{-3}$)	$\sim10^6$	1.5×10^{-4} ($\pm1\times10^{-4}$)	$\sim10^3$	2.3×10^{-2} ($\pm0.2\times10^{-2}$)	$\sim4\times10^3$
p-xylene (b.p. 138 °C)	1.5×10^{-2} ($\pm0.4\times10^{-2}$)	$\sim10^4$	1.4×10^{-3} ($\pm0.5\times10^{-3}$)	$\sim10^2$	1.5×10^{-2} ($\pm0.2\times10^{-2}$)	$\sim3\times10^3$
Chloroform (b.p. 61 °C)	8.5×10^{-2} ($\pm2\times10^{-2}$)	$\sim5\times10^4$	2.1×10^{-2} ($\pm0.3\times10^{-2}$)	$\sim10^3$	1.1×10^{-3} ($\pm0.3\times10^{-3}$)	$\sim10^3$
Chloroform on HMDS-treated SiO_2	1.5×10^{-1} ($\pm0.2\times10^{-1}$)	$\sim2\times10^5$	2.3×10^{-3} ($\pm0.2\times10^{-3}$)	$\sim10^3$	1.6×10^{-3} ($\pm0.4\times10^{-3}$)	$\sim10^4$

Downloaded 15 Aug 2006 to 131.155.214.50. Redistribution subject to AIP license or copyright, see http://jap.aip.org/jap/copyright.jsp

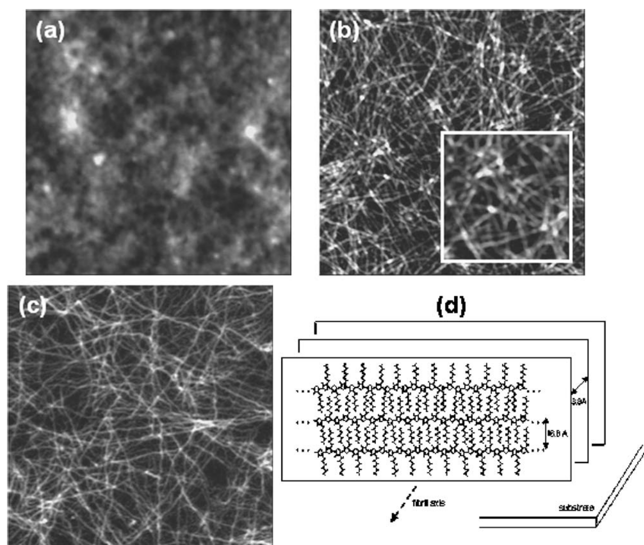

FIG. 2. TM-AFM 2×2 μm^2 height images (vertical grayscale=20 nm) within the FET channel for deposits prepared by dip coating: (a) from 1,2,4-TCB; (b) from *p*-xylene (inset: 600×600 nm^2 zoom image); (c) from chloroform. (d): Schematic representation of the crystallization of RR-P3HT chains into one fibril (one dimensional-lamella), due to π stacking of the conjugated backbones and the interdigitation of the alkyl groups.

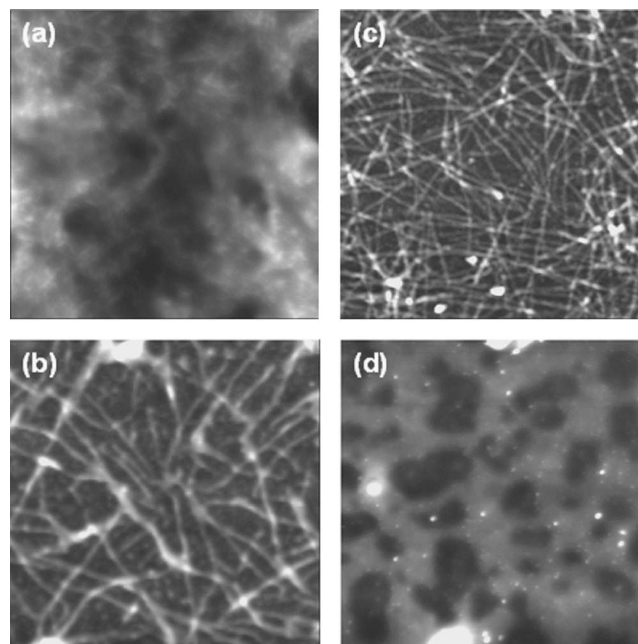

FIG. 3. TM-AFM 2×2 μm^2 height images (vertical grayscale=20 nm) within the channel of FETs prepared: Left: drop-cast films: (a) from 1,2,4-TCB; (b) from *p*-xylene. Right: spin-coated films: (c) from *p*-xylene; (d) from chloroform.

groups),[17] as depicted schematically in Fig. 2(d). The width and height of the fibrils are consistent with such a packing structure, since the average chain length for a fully extended molecule is estimated to be roughly on the order of the width of the fibrils (contour length around 20–30 nm)[18] while the height in the short axis (along the interlamellar axis) is a few nm, i.e., few stacked lamellae. It is worth pointing out that films of regiorandom P3HT, which does not crystallize, do not exhibit fibrillar structures, regardless of the film deposition method used.[19]

The fibrillar structure appears to give rise to relatively high charge mobility, in the 10^{-2}–10^{-1} cm^2 V^{-1} s^{-1} range, while films made from TCB/polymer solutions, which lack the above structural order, show mobilities around 10^{-3} cm^2 V^{-1} s^{-1}. Since the fibrils are the result of strong intermolecular interactions between adjacent conjugated backbones, the charge hopping rate is large compared to that in amorphous structures (in which the chains poorly interact).[20] Moreover, the fibrils are a few μm long, i.e., on the order of the channel length, and therefore can act as efficient paths for enhanced charge transport. Note that recently Frisbie *et al.* have measured the electrical properties of a single fibril of RR-P3HT,[21] and deduced a carrier mobility around 10^{-2} cm^2 V^{-1} s^{-1}, which is compatible with our results. These authors proposed that, in those fibrils, the charge transport is limited by the presence of traps, which are probably located at the domain boundaries between amorphous and crystalline regions and/or arise due to conformational defects (e.g., head-to-head linkages).

There is little difference in terms of microstructure between dip-coated films from *p*-xylene (μ=0.015 cm^2 V^{-1} s^{-1}) and chloroform (μ=0.085 cm^2 V^{-1} s^{-1}) except their root mean square (rms) roughness, as determined from AFM image analysis.[22] Deposits from chloroform exhibit a rms roughness of 3.1 nm while for those made from *p*-xylene are slightly rougher (rms roughness around 4.2 nm). This difference is probably due to the presence of small grains in the case of deposits from *p*-xylene [see Fig. 2(b) inset], which can decrease the mobility because of traps located at the grain boundaries. In contrast, no such granular defects are found for films made using dip coating from chloroform, which exhibit well-defined fibrils and the highest mobility value reported in our experiments.

Drop-cast films show relatively poor performances, both in terms of charge mobility (10^{-4}–10^{-3} cm^2 V^{-1} s^{-1}) and current on/off ratio ($\sim 10^3$), most probably as a consequence of the noncomplete coverage of the channel and/or the amorphous structure of the films [see Fig. 3(a)]. Even if bundles of fibrils are present (in the case of deposits from *p*-xylene [Fig. 3(b)], they only partially cover the silicon oxide dielectric substrate. The relatively good charge mobility for deposits from chloroform (0.021 cm^2 V^{-1} s^{-1}) can arise from the relatively high structural order characterized by a fibrillar texture with fibrils 15–20 nm wide. This finding is in agreement with the studies of Yang *et al.*,[14] who showed that the use of chloroform leads to higher FET carrier mobility in drop-cast films due to the higher crystalline order (as studied by x-ray diffraction), compared to that observed in FET made with higher boiling point solvents, such as toluene.

Interestingly, an opposite trend was observed for spin-coated films: films prepared using higher boiling solvents show higher performance, in agreement with the observations of Chang *et al.*[9] In this case, deposition from chloroform leads to smooth, untextured films with large holes [Fig. 3(d)], which resulted in low carrier mobility (10^{-4} cm^2 V^{-1} s^{-1}), while films prepared from both *p*-xylene and TCB display a fibrillar structure and a mobility larger than 10^{-2} cm^2 V^{-1} s^{-1}. We note that films prepared from

Downloaded 15 Aug 2006 to 131.155.214.50. Redistribution subject to AIP license or copyright, see http://jap.aip.org/jap/copyright.jsp

p-xylene show a similar microstructure, whether they were prepared by dip coating or spin coating (shown in Fig. 3), and indeed similar FET performances.

Having described how the microscopic morphology dramatically influences the polymer FET performance, the question arises as to how the various preparation techniques lead to such different microstructures, even when the same solvent is used. These observations can be rationalized in the following way:

(i) For dip coating and drop casting, the quality of the film depends on the solvent evaporation rate. Thus, when using solvents with relatively slow evaporation rate (slow film formation), it appears likely that other processes operate before the crystallization, such as dewetting of the solvent on the substrate and amorphous assembly of RR-P3HT chains. That is the case for thin drop-cast films from *p*-xylene and TCB, which do not cover the substrate (e.g., the FET channel) well, due to unfavorable interfacial interaction between solvent and substrate.

(ii) In the case of spin coating, the film formation is influenced both by the solvent evaporation process and by the spinning speed (and the viscosity of the solution). At speeds generally used to prepare thin polymer films (>1000 rpm), the rapid spreading of the solvent appears to accelerate its evaporation, which in the case of chloroform prevents crystallization. In contrast, for solvents evaporating more slowly, crystallites can be formed during the somewhat longer time available for the "mobile" polymer chains in solution to crystallize. Moreover, the spin-coating process "forces" a uniform thin liquid layer to form due to high-speed rotation, and therefore preventing the occurrence of dewetting.

Altogether, these results highlight that the microscopic morphology is sensitively dependent on the interplay between the crystallization rate of the RR-P3HT chains and the evaporation rate of the solvent, processes that can be manipulated by the choice of the processing technique and the solvent. The dip-coating technique seems to yield the best performances because it allows for the formation of a fibrillar structure (crystalline lamellae). Note that the dipping direction with respect to the electrode orientation did not affect the final device performance, as the fibrils appear to be randomly oriented in the FET channel. Moreover, a careful AFM investigation of the interface with the gold electrodes showed that the fibrils, although being only a few nm thick, are continuous over the channel-electrode interface, despite the fact that the electrodes are by far thicker (around 50 nm thick, as deduced from the phase image in Fig. 4). Note that, for a given solvent and processing condition, we observe the same morphology on the two different surfaces (SiO_x channels and Au electrodes), confirming the fact that the solvent drives the film morphology.

In order to further improve the device performance, many groups have adopted a procedure of coating the silicon oxide dielectric with self-assembled monolayers (SAMs) that change the nature of the dielectric substrate (or using other polymeric dielectric layers).[23] For example, by incorporating SAMs, tuning of the surface polarity of the gate insulator could be achieved by the choice of the terminal end groups;[24] this includes, for instance, hexamethyldisilazane (HMDS) or trichlorosilanes, which react with the silanol (Si–O–H) groups and form Si–O–Si–C bonds at the surface. In our studies we have used HMDS in order to convert the rather polar surface into a nonpolar one.

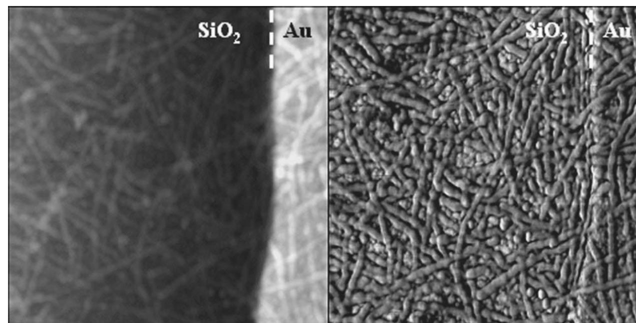

FIG. 4. TM-AFM height (left) and phase (right) 1.5×1.5 μm^2 images of dip-coated films from *p*-xylene, at the Au–SiO_2 interface.

Untreated silicon oxide (SiO_2) is typically characterized by a relatively rough, granular surface with a rms roughness of 2.1 nm. The HMDS-treated SiO_2 has a somewhat rougher surface than SiO_2, due to the presence of islands of the HMDS on the surface (rms roughness of 3.3 nm). The FET performance depends on the deposition method and the solvent: for instance, *p*-xylene and TCB do not wet (cover) properly the SiO_2 treated with HMDS, and the droplets formed resulted either in nonworking or poorly working FETs. For dip-coated and spin-coated films from chloroform solutions on HMDS-treated SiO_2, the charge mobility and the on/off ratios are generally better than those for drop-cast films. Note that dip-coated films prepared from chloroform onto HMDS-treated substrates displayed similar morphology as devices made using pristine SiO_2, i.e., a well-defined fibrillar morphology. Therefore, the slight increase in carrier mobility and on/off current ratio in this case (see Table I, last row) is not attributed to morphological changes but to the decrease in the density of carrier traps at the SiO_2/polymer interface and possibly to the change in the local polarization which may affect the extent of charge carrier localization at the interface, as several studies have established that nonpolar and defect-free interfaces result in significantly improved OFET characteristics.[25] Notice that, in contrast to the above cases, drop-cast films display a reduced carrier mobility of about one order of magnitude compared to that in devices prepared on pristine SiO_2 gate dielectric.

A further improvement of the device performance was achieved by thermally annealing the RR-P3HT layer with the optimal fabrication conditions as described above; for example, FETs prepared using dip coating of the HMDS-treated SiO_2 substrates in polymer/chloroform solution were subsequently annealed on a hot plate at controlled temperature in a nitrogen atmosphere, in order to reduce oxidative contamination as described in detail by Cho *et al.*[26] The mobility gradually increasing from 0.15 $cm^2\,V^{-1}\,s^{-1}$ for the nonannealed device to almost 0.25 $cm^2\,V^{-1}\,s^{-1}$ for the annealed

Downloaded 15 Aug 2006 to 131.155.214.50. Redistribution subject to AIP license or copyright, see http://jap.aip.org/jap/copyright.jsp

device at 150 °C. Annealing at this temperature probably improves the crystallinity within the fibrils, which enhances the interchain interactions and consequently the charge mobility.

IV. CONCLUDING REMARKS

Our studies provide an insight into the interplay between the charge transport, the microscopic morphology, and the film preparation methods of high-performance FET using RR-P3HT. We have shown how the microstructure of the RR-P3HT thin FET active layer influences the device performance. The solvent used in the polymer film deposition as well as the deposition method determine the film microstructure, which ranges from amorphous or granular films to a well-defined fibrillar texture. The crystalline order of RR-P3HT and the formation of the fibrillar structure appear to lead to optimal FET performances, suggesting that fibrils act as efficient paths for the charge carrier transport. This conclusion is in agreement with the relationship between FET performance and the mesoscale crystalline structure of RR-P3HT (in studies on drop-cast films using X-ray diffraction) recently reported by Yang *et al.*,[14] at variance with the conclusions of Kline *et al.*,[12] who suggested that the fibrillar structures are detrimental for charge transport. The dip-coating process appears to provide the best FET performances in our studies, with hole mobility approaching 10^{-1} cm V^{-1} s^{-1} and current on/off ratio of $\sim 10^5$, i.e., values that demonstrate the potential of RR-P3HT for low-cost FET device applications.

ACKNOWLEDGMENTS

The research at UCSB was supported by the Samsung Advanced Institute of Technology. Part of this work made use of MRL Central Facilities supported by the MRSEC Program of the National Science Foundation under Award No. DMR05-20415. S.C. acknowledges the support by the Korea Research Foundation Grant No. M07-2004-000-10137-0 and M.S. acknowledges the F.R.I.A. (Belgium) for a doctoral fellowship and Communauté française de Belgique for a research stay grant. Ph.L. is Chercheur Qualifié of the "Fonds National de la Recherche Scientifique" (FNRS-Belgium).

[1](a) C. D. Dimitrakopoulos and P. R. L. Malenfant, Adv. Mater. (Weinheim, Ger.) **14**, 99 (2002); (b) G. Horowitz, J. Mater. Res. **19**, 1946 (2004).
[2](a) G. Horowitz, Adv. Mater. (Weinheim, Ger.) **10**, 365 (1998); (b) F. Dinelli, M. Murgia, P. Levy, M. Cavallini, F. Biscarini, and D. M. De Leeuw, Phys. Rev. Lett. **92**, 116802 (2004).
[3](a) R. D. McCullough, Adv. Mater. (Weinheim, Ger.) **10**, 93 (1998); (b) T.-A. Chen, X. Wu, and R. D. Rieke, J. Am. Chem. Soc. **117**, 233 (1995).
[4]H. Sirringhaus, P. J. Brown, R. H. Friend, M. M. Nielsen, K. Bechgaard, B. M. W. Langeveld-Voss, A. J. H. Spiering, R. A. J. Janssen, E. W. Meijer, P. Herwig, and D. M. de Leeuw, Nature (London) **401**, 685 (1999).
[5]G. Wang, J. Swensen, D. Moses, and A. J. Heeger, J. Appl. Phys. **93**, 6137 (2003).
[6](a) L. Zhai and R. D. McCullough, Adv. Mater. (Weinheim, Ger.) **14**, 901 (2002); (b) N. Reitzel, D. R. Greve, K. Kjaer, P. B. Howes, M. Jayaraman, S. Savoy, R. D. McCullough, J. T. McDevitt, and T. Bjørnholm, J. Am. Chem. Soc. **122**, 5788 (2002); (c) J. Locklin, J. H. Youk, C. Xia, M.-K. Park, X. Fan, and R. C. Advincula, Langmuir **18**, 877 (2002); (d) X. L. Chen, A. J. Lovinger, Z. Bao, and J. Sapjeta, Chem. Mater. **13**, 1341 (2001); (e) H. G. O. Sandberg, G. L. Frey, M. N. Shkunov, H. Sirringhaus, R. H. Friend, M. M. Nielsen, and C. Kumpf, Langmuir **18**, 10176 (2002).
[7]B. S. Ong, Y. Wu, P. Liu, and S. Gardner, Adv. Mater. (Weinheim, Ger.) **17**, 1141 (2005).
[8](a) G. Horowitz, X.-Z. Peng, D. Fichou, and F. Garnier, Synth. Met. **51**, 419 (1992); (b) G. Wang, D. Moses, A. J. Heeger, H.-M. Zhang, M. Narasimhan, and R. E. Demaray, J. Appl. Phys. **95**, 316 (2004); (c) D. H. Kim, Y. D. Park, Y. Jang, H. Yang, Y. H. Kim, I. J. Han, D. G. Moon, S. Park, T. Chang, C. Chang, M. Joo, C. Y. Ryu, and K. Cho, Adv. Funct. Mater. **15**, 77 (2005).
[9]J.-F. Chang, B. W. Sun, D. Breiby, M. M. Nielsen, T. I. Solling, M. Giles, I. McCulloch, and H. Sirringhaus, Chem. Mater. **16**, 4772 (2004).
[10]Z. Bao, A. Dodabalapur, and A. J. Lovinger, Appl. Phys. Lett. **69**, 4108 (1996).
[11]B. S. Ong, Y. Wu, P. Liu, and S. Gardner, J. Am. Chem. Soc. **126**, 3378 (2004).
[12]R. J. Kline, M. D. McGehee, E. N. Kadnikova, J. Liu, and J. M. J. Fréchet, Adv. Mater. (Weinheim, Ger.) **15**, 1519 (2003).
[13]G. Wang, T. Hirasa, D. Moses, and A. J. Heeger, Synth. Met. **146**, 127 (2004).
[14]H. Yang, T. J. Shin, L. Yang, K. Cho, C. Y. Ryu, and Z. Bao, Adv. Funct. Mater. **15**, 671 (2005).
[15]L.-L. Chua, J. Zaumseil, J. F. Chang, E. C.-W. Ou, P. K.-H. Ho, H. Sirringhaus, and R. H. Friend, Nature (London) **434**, 194 (2005).
[16](a) H. Yang, S. Park, D. Kim, K. Oh, S. Magonov, K. Cho, T. Chang, Z. Bao, and C. Y. Ryu, Polym. Prepr. (Am. Chem. Soc. Div. Polym. Chem.) **44**, 333 (2003); (b) H. Yang, T. J. Shin, L. Yang, Z. Bao, C. Y. Ryu, and K. Cho, *ibid.* **45**, 212 (2004).
[17]A. Zen, J. Pflaum, S. Hirschmann, W. Zhuang, F. Jaiser, U. Asawapirom, J. P. Rabe, U. Scherf, and D. Neher, Adv. Funct. Mater. **14**, 757 (2004).
[18]The average molecular weight is given as $\langle M_n \rangle = 25\,500$ g/mol and $\langle M_w \rangle = 37\,680$ g/mol, respectively, as determined using GPC with PS standards [Ref. 3(b)]. This method introduces an overestimation of the molecular weight by a factor of 2 to 3, due to the rigid nature of the conjugated chains, see, e.g., (a) J. Liu, R. S. Loewe, and R. D. McCullough, Macromolecules **32**, 5777 (1999). See also the estimation of the contour length of RR-P3HT using STM: B. Grévin, P. Rannou, R. Payerne, A. Pron, and J. P. Travers, J. Chem. Phys. **118**, 7097 (2003).
[19]G. Derue, S. Coppée, S. Gabriele, M. Surin, V. Geskin, F. Monteverde, Ph. Leclère, R. Lazzaroni, and P. Damman, J. Am. Chem. Soc. **127**, 8018 (2005).
[20]J. Cornil, D. Beljonne, J. P. Calbert, and J. L. Brédas, Adv. Mater. (Weinheim, Ger.) **13**, 1053 (2001).
[21]J. A. Merlo and C. D. Frisbie, J. Polym. Sci., Part B: Polym. Phys. **41**, 2674 (2003); J. A. Merlo and C. D. Frisbie, J. Phys. Chem. B **108**, 19169 (2004).
[22]The rms roughness is the standard deviation of the height values with respect to the average height.
[23]For recent reviews on gate insulators used in OFETs, see: (a) J. Veres, S. Ogier, G. Lloyd, and D. de Leeuw, Chem. Mater. **16**, 4543 (2004); (b) A. Facchetti, M.-H. Yoon, and T. J. Marks, Adv. Mater. (Weinheim, Ger.) **17**, 1705 (2005).
[24]D. H. Kim, Y. Jang, Y. D. Park, and K. Cho, Langmuir **21**, 3203 (2005).
[25]J. Veres, S. D. Ogier, S. W. Leeming, D. C. Cupertino, and S. M. Khaffaf, Adv. Funct. Mater. **13**, 199 (2003).
[26]S. Cho, J. Yuen, G. Wang, D. Moses, K. Lee, A. J. Heeger, M. Surin, and R. Lazzaroni, J. Appl. Phys.(submitted).

Downloaded 15 Aug 2006 to 131.155.214.50. Redistribution subject to AIP license or copyright, see http://jap.aip.org/jap/copyright.jsp